fluids

MDPI

Article

Rapid Assessment of Relative Hemolysis Amidst Input Uncertainties in Laminar Flow

Nasim Gholizadeh [1], Ryan Wang [2], Gayatri Gautham [2] and Gautham Krishnamoorthy [1,*]

[1] Department of Chemical Engineering, University of North Dakota, UPSON II Room 365, 241 Centennial Drive, Grand Forks, ND 58202, USA; nasim.gholizadeh@und.edu
[2] Red River High School, 2211 17th Ave S, Grand Forks, ND 58201, USA; ryanwang4545@gmail.com (R.W.); gayatrigautham7@gmail.com (G.G.)
* Correspondence: gautham.krishnamoorthy@und.edu; Tel.: +1-701-777-6699

Abstract

Predicting *absolute* values of hemolysis using the power law model to guide medical device design is hampered by uncertainties stemming from four sources of model inputs: incoming/upstream velocity profiles, blood viscosity models, power law hemolysis coefficients, and obtaining accurate stress exposure times. Amidst all these uncertainties, enabling rapid assessments and predictions of *relative* hemolysis would still be valuable for evaluating device design prototypes. Towards achieving this objective, hemolysis data from the Eulerian modeling framework was first generated from computational fluid dynamics simulations encompassing five blood viscosity models, four sets of hemolysis power law coefficients, fully developed as well as developing velocity flow conditions, and a wide range of shear stresses, strain rates, and stress exposure times. Corresponding hemolysis predictions were also made in a Lagrangian framework via numerical integration of shear stress and residence time spatial variations under the assumption of fully developed Newtonian fluid flow. *Absolute* hemolysis predictions (from both frameworks) were proportional to each other and independent of the blood viscosity model. Further, *relative* hemolysis trends were not dependent on the hemolysis power law coefficients. However, accuracy in wall shear stresses in developing flow conditions is necessary for accurate *relative* hemolysis assessments.

Keywords: hemolysis; power law model; non-newtonian; laminar; uncertainty

check for updates

Academic Editors: Chengcheng Tao and Mehrdad Massoudi

Received: 22 July 2025
Revised: 20 August 2025
Accepted: 27 August 2025
Published: 29 August 2025

Citation: Gholizadeh, N.; Wang, R.; Gautham, G.; Krishnamoorthy, G. Rapid Assessment of Relative Hemolysis Amidst Input Uncertainties in Laminar Flow. *Fluids* **2025**, *10*, 228. https://doi.org/10.3390/fluids10090228

Copyright: © 2025 by the authors. Licensee MDPI, Basel, Switzerland. This article is an open access article distributed under the terms and conditions of the Creative Commons Attribution (CC BY) license (https://creativecommons.org/licenses/by/4.0/).

1. Introduction

Hemolysis, the destruction of red blood cells (RBC) caused by non-physiological stresses in blood-contacting medical devices, is a major concern for patient safety. Exposure to low shear stress and long exposure time can substantially damage the red blood cells, leading to biochemical changes. Similarly, high shear stress but short exposure time can cause instantaneous rupture of the blood cells due to mechanical forces. Therefore, designing blood-contacting devices that mitigate hemolysis through appropriate flow control strategies is of interest. In support of this effort, hemolysis of blood has been studied in geometries ranging from straight capillary tubes [1] (cf. Figure 1a) to idealized benchmark geometries such as the generic Food and Drug Administration (FDA) benchmark nozzle model (cf. Figure 1b,c) [2–5].

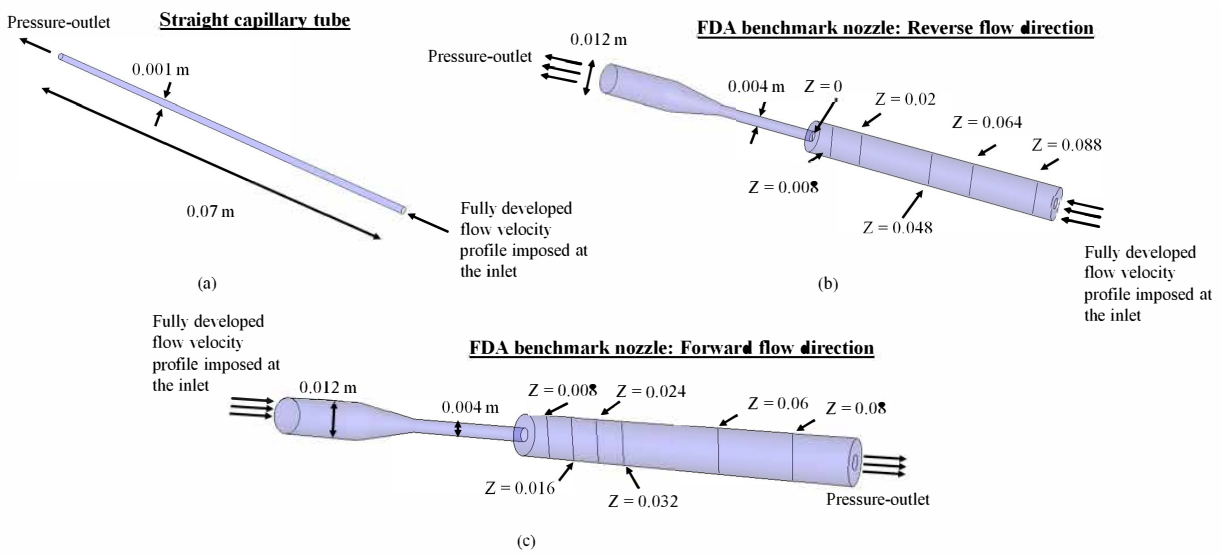


Figure 1. Geometries examined in this study: (**a**) straight capillary tube (Kameneva et al. [1]); (**b**) reverse flow in the bidirectional FDA benchmark nozzle; (**c**) forward flow in the bidirectional FDA benchmark nozzle.

However, even after standardizing experimental protocols for generating benchmark measurement data, significant measurement and computational fluid dynamics (CFD)-based prediction variability was observed in the data presented in inter-/multi-laboratory studies of these geometries [2–5]. Further, recent studies have assessed the universal applicability of the commonly employed hemolysis power law model to quantify blood damage [6] and even highlighted prediction variations resulting from implementing this model in Eulerian and Lagrangian frameworks [7]. Even by restricting ourselves to the laminar flow conditions associated with the geometries shown in Figure 1, the measured and predicted variabilities in flow and hemolysis characteristics appear to stem from four main sources of uncertainty shown in Figure 2. Amidst all these uncertainties, a recent conclusion regarding the practical/clinical utility of hemolysis modeling appears to be that while current hemolysis modeling frameworks cannot predict the absolute values of hemolysis, it might be possible to predict their *relative* values in different flow and device configurations [6].

In light of this recent conclusion, the goal of this paper is to enable rapid assessments and predictions of *relative* hemolysis towards quickly evaluating device design prototypes. The investigated scenarios include: three flow configurations (cf. Figure 1) for investigating *inlet velocity profile variability/uncertainty* (well defined inlet velocities associated with fully developed flow conditions in the straight capillary tube to spatially varying incoming velocity profiles at the throat section of the FDA nozzle throat that is governed by the flow direction), five blood viscosity models (Table 1) for *blood viscosity model uncertainty/sensitivities*, and four sets of hemolysis power law constants (Table 2) for *power law coefficients uncertainty/sensitivities* employed in both *Eulerian/Lagrangian model framework uncertainties*. We specifically restrict ourselves to laminar flow conditions for the following reasons: The average Reynolds number (Re) stays within the laminar regime in many anatomical regions within the human body [8]. Blood is a shear-thinning fluid that approaches Newtonian behavior at high strain rates; therefore, the effects of and differences between Non-Newtonian models are expected to become more pronounced at the lower strain rates associated with laminar flow conditions. Furthermore, the impact of any turbulence modeling uncertainties on our predictions and conclusions is avoided. Also, the turbulent Reynolds stresses that are predicted in Reynolds Average Navier Stokes

(RANS) turbulence modeling approaches do not directly correspond to the real mechanical or physical stress experienced by the RBC.

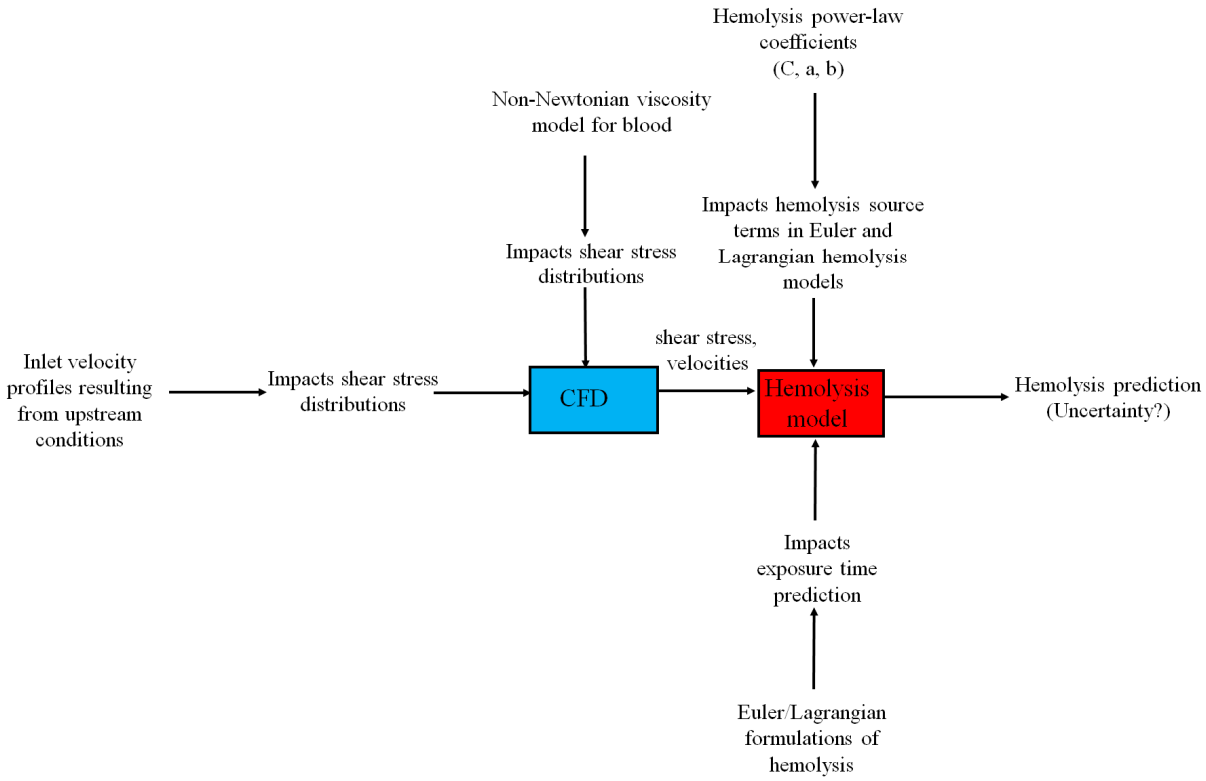


Figure 2. Sources of uncertainty in hemolysis prediction under laminar flow conditions.

Table 1. Viscosity (μ) versus shear rate $(\dot{\gamma})$ and their coefficients utilized to evaluate the Non-Newtonian behavior of the fluid (blood) based on Kopernik [9].

Type	Viscosity Model	Constants
Carreau–Yasuda (CY)	$\mu = \mu_\infty + (\mu_0 - \mu_\infty)\left[1 + (\lambda\dot{\gamma})^\alpha\right]^{\frac{n-1}{\alpha}}$	$\mu_\infty = 0.0035$ Pa·s $\mu_0 = 0.056$ Pa·s $\lambda = 1.902$ $\alpha = 1.25$ $n = 0.22$
Casson	$\mu = \frac{\mu_\infty^2}{\dot{\gamma}} + \frac{2\mu_\infty N_\infty}{\sqrt{\dot{\gamma}}} + N_\infty^2$ $N_\infty = \frac{\sqrt{\mu_p}}{\sqrt[8]{1-Hct}}$ $\mu_\infty = \sqrt{0.625\ Hct}$	$\mu_p = 0.00145$ $Hct = 0.4$
Cross	$\mu = \mu_\infty + \frac{\mu_0 - \mu_\infty}{1+\left(\frac{\dot{\gamma}}{\gamma_c}\right)^n}$	$\mu_\infty = 0.0035$ Pa·s $\mu_0 = 0.0364$ Pa·s $\gamma_c = 2.63\ s^{-1}$ $n = 1.45$
Power Law	$\mu_{min} < \mu = \lambda\lvert\dot{\gamma}\rvert^{n-1} < \mu_{max}$	$n = 0.7755$ $\lambda = 0.01467$ $\mu_{\max} = 0.025$ Pa·s $\mu_{min} = 0.00345$ Pa·s

Table 2. Hemolysis constants associated with the blood damage index D, which is expressed as a function of shear stress (τ) and exposure time (t) as $D = C\tau^b t^a$.

Model Name	Constants Source	a	b	C
Blood damage I	Giersiepen et al. [10]	0.785	2.416	3.620×10^{-7}
Blood damage II *	Craven et al. [11] (ξ = 0.5)	0.5	2.65	2.88×10^{-10}
Blood damage III *	Craven et al. [11] (ξ = 0.75)	0.7375	2.9	1.81×10^{-10}
Blood damage IV *	Craven et al. [11] (ξ = 1.0)	1.0	3.1	1.5×10^{-10}

* ξ is a parametric variable employed to estimate the hemolysis constants in Craven et al. [11].

The specific contributions of this study regarding the four sources of uncertainties delineated above are detailed below.

1.1. Assessing Prediction Sensitivity to Inflow Velocity Profiles

The incoming velocity profile at the inlet of a medical device is governed by the upstream geometry. Experimental measurements showed that even at laminar conditions, for a throat Reynolds number (Re_t) of 2000, the size and the velocity of the jet in the sudden expansion region downstream of the throat in the FDA nozzle (cf. Figure 1c) were very sensitive to the inflow (upstream) conditions [2]. Further, CFD predicted shear stress distributions, particularly the wall shear stress distributions, which also showed significant variations in laminar regimes [3,4]. This has particular relevance and impact for developing shear-induced blood damage models since not only are the shear stresses high in the near-wall region, but the RBC exposure time is also high due to lower near-wall velocities. A medical device such as a ventricular assist device may also have very short and/or curved entrance and exit conduits, and an accurate inlet velocity profile specification may be necessary to capture the flow and hemolysis characteristics within the device accurately. Within the FDA nozzle, at identical Re_t, the direction of flow (forward/reverse cf. Figure 1b,c) has been shown to have a significant impact on the hemolysis under turbulent conditions [5]. Hemolysis was exacerbated in the reverse flow direction (cf. Figure 1b) due to flow impingement when the geometry transitions from the sudden expansion section to the throat. However, the impact on flow direction under laminar conditions in the FDA geometry has not been assessed, where most of the hemolysis is anticipated to occur at the throat [3,4].

Contribution #1 of this study: The first goal of this study is to assess the impact of this uncertainty/variations in upstream inlet velocity profiles on the relative hemolysis at the throat. This is undertaken by comparing CFD-based hemolysis predictions in the bidirectional FDA nozzle for flow directions shown in Figure 1b,c using an Eulerian representation of the hemolysis power law model. Blood flow in the human body is pulsatile. However, temporal variations in inflow velocity profiles are not considered here since pulsatile or time-dependent inflow boundary conditions have been shown to have a minimal impact on the time-averaged wall shear stress predictions within the FDA nozzle [12,13]. While Stiem et al. [12] showed distinct differences between time-averaged axial velocity profiles generated from constant velocity and pulsatile velocity inflow boundary conditions downstream of the throat in the forward flow direction (cf. Figure 1c), these differences did not manifest themselves for derived quantities like shear stresses. Therefore, only steady-state laminar flow simulations are performed in this study.

1.2. Prediction Sensitivity to Blood Viscosity Models

Blood is a shear-thinning fluid with significant viscosity variations at low shear rates. Different viscosity models have been proposed to model this behavior of blood and are summarized in Table 1. The shear thinning viscosity predicted by the different models is shown in Figure 3.

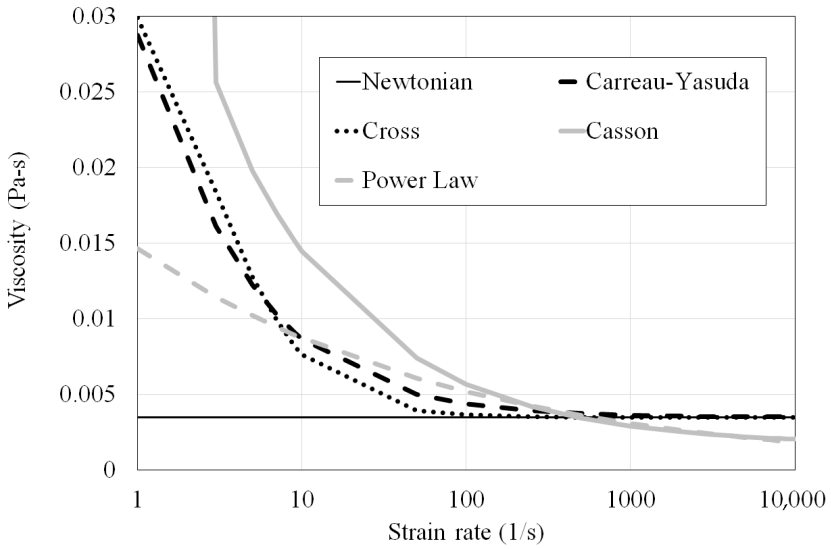


Figure 3. Viscosity variations employing the different Non-Newtonian models for blood investigated in this study. A constant viscosity of 0.0035 Pa-s (shown) was used in the FDA nozzle geometry.

The significant variations in viscosity among the models observed at low strain rates (<100 s^{-1}) in Figure 3 imply that the choice of the viscosity model may significantly impact the velocity and shear stress profiles and consequently hemolysis predictions at laminar flow conditions. Indeed, Trias et al. [14] observed up to 10% differences in velocity, pressure, and shear stress fields between Newtonian and Non-Newtonian models (Casson, Carreau, Yasuda) and a 17% difference in hemolysis predictions at Re_t = 500 in the FDA nozzle geometry. Similarly, Good [13] analyzed Newtonian and Non-Newtonian models (Casson and Carreau) under steady and pulsatile flows in the FDA nozzle, finding notable differences in recirculation patterns, pressure drop, and throat velocities, particularly at Re_t = 500. Significant influences of viscosity models on wall shear stress and velocity distributions at Re_t = 500 have been observed in other studies as well [15,16]. Our recent study showed significant prediction variations in blood damage (by nearly a factor of six) among the Non-Newtonian models at Re_t = 500 associated with forward flow in the bidirectional FDA nozzle (cf. Figure 1c) [17].

Contribution #2 of this study: Previous studies have confirmed that for laminar flow within the FDA nozzle, the regions of highest shear stress [3,4] and highest hemolysis rates occur at the throat at Re_t < 2000 [14,17]. Previous studies have also shown that Non-Newtonian fluids have similar shear stress characteristics as Newtonian fluids [18] in round pipe geometries and fully developed flow conditions. Therefore, it is important to assess if the hemolysis prediction differences between Newtonian and Non-Newtonian fluids within the FDA nozzle observed previously [14,17] were only being exacerbated due to differences in the incoming velocity profiles that are a function of upstream geometry features. In order to delineate between the inlet velocity profile and viscosity effects, hemolysis predictions within the FDA nozzle employing different Non-Newtonian models will be carried out for both flow directions (cf. Figure 1b,c). The impact of flow direction/inlet velocity profiles will then be individually assessed for each viscosity model. In addition, Non-Newtonian models will be employed to predict hemolysis in the straight capillary tube (cf. Figure 1a)

with well-defined, fully developed velocity profiles imposed at the inlet to assess the impact of the viscosity model alone on the hemolysis.

1.3. Prediction Sensitivity to Hemolysis Power Law Constants

The relationship between flow-induced mechanical stress and red blood cell (RBC) damage is often expressed in terms of a hemolysis power law model, where the blood damage index D is expressed as a function of shear stress (τ) and exposure time (t) as:

$$D = C\tau^b t^a \tag{1}$$

where C, b, and a are empirically derived coefficients generally obtained from measurements in Couette-type blood shearing devices with uniform-shear, laminar conditions, and well-defined exposure times [11]. While D in Equation (1) can be computed in a Lagrangian framework by tracking τ and t along multiple pathlines/streamlines and obtaining a mass-weighted summation/average, a corresponding Eulerian representation of Equation (1) is obtained by solving a scalar transport equation for the time-linearized damage field D_e as:

$$\frac{\partial(\rho D_e)}{\partial t} + \nabla(\rho D_e v) = C^{\frac{1}{a}}\rho|\tau|^{\frac{b}{a}} \tag{2}$$

where the dependency on the exposure time (which is not directly available in an Eulerian framework) is built into the time linearized blood damage index D_e as $D_e = D^{1/a}$. The erroneous approximations associated with generalizing this approach in simple geometries have been discussed by Faghih et al. [7], especially when there are large regions of flow acceleration and recirculation. The Eulerian and Lagrangian approximations are also compared in this study in the context of relative hemolysis predictions in the more complex bidirectional FDA nozzle. The constants of Giersiepen et al. [10] were used by Trias et al. [14] and Krishnamoorthy and Gholizadeh [17] to assess damage due to Non-Newtonian flows in the FDA nozzle and are also used in the FDA nozzle simulations in this study. Device-specific coefficients for the Kameneva et al. [1] geometry were derived by Craven et al. [11] but were expressed in terms of the parametric variable ξ, (with $0 \leq \xi \leq 1$) and are used in the capillary tube portion of this study for ξ, values of 0.5, 0.75, and 1.0, respectively. Just to give a sense of the magnitude of absolute hemolysis variability resulting from the use of these constants, the source term of Equation (2) is shown in Figure 4 as a function of shear stress for the hemolysis constants employed in this study. A three orders of magnitude variation is seen across the range of shear stresses (<600 Pa) associated with this study.

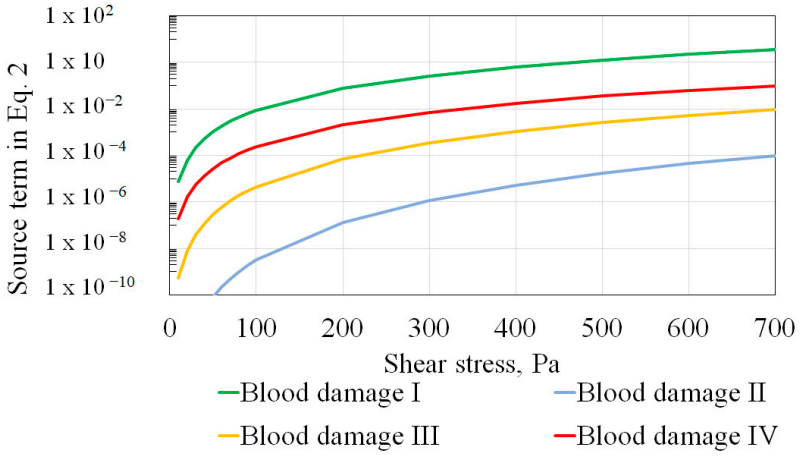


Figure 4. Source term magnitude (right-hand side of equation) in Equation (2) variations as a function of shear stress.

Contribution #3 of this study: The fact that hemolysis power law constants obtained from blood shearing devices are device-specific as well as blood sample-specific has been well recognized [6,11]. Furthermore, given the wide variations in the source term magnitude shown in Figure 4, there is now consensus that the absolute values of hemolysis cannot be predicted accurately using the power law formulation in the absence of device and blood sample-specific coefficients. Given this shortcoming, this study explores the ability to predict relative hemolysis in the straight capillary tube geometry (cf. Figure 1a) for different choices of power law coefficients (Table 2). The simulations are carried out employing all of the viscosity models (Table 1) and the relative hemolysis rates (i.e., absolute hemolysis versus shear stress variations) are assessed. In addition, fully developed velocity profiles are maintained at the inlet, thereby enabling us to delineate the effects of hemolysis power law coefficient variations alone.

1.4. Prediction Sensitivity to Eulerian and Lagrangian Formulations of the Hemolysis Power Law

The fact that Eulerian representation results in erroneous residence time when there is flow acceleration or recirculation has been well recognized [7]. However, it may be difficult to obtain a converged solution using the Lagrangian formulation due to the need to generate an adequate number of pathlines within a complex device geometry. In lieu of this, an analytical solution to the blood damage index will be estimated via numerical integration of shear stress and residence time spatial variations under the assumption of fully developed Newtonian fluid flow. The absolute hemolysis values in both Eulerian and this simplified Lagrangian framework are compared and their ability to predict relative hemolysis rates is assessed.

Contribution #4 of this study: Recent studies [7] have suggested that since the erroneous treatment of residence time in the Eulerian formulation (resulting from flow acceleration) may necessitate the formulation/deduction of separate sets of coefficients for each (Eulerian/Lagrangian) formulation, our goal is to explore if this requirement may be alleviated for relative hemolysis assessments.

2. Methods

The steady-state computational fluid dynamics (CFD) simulations were carried out using ANSYS FLUENT version 2023R2 [18]. The incompressible Navier–Stokes equations (Equations (3) and (4)) were used to calculate velocity profiles. The steady state mass conservation equation shown in Equation (3) was used in conjunction with the momentum conservation equation (Equation (4)) for carrying out the calculations.

$$\nabla \cdot (\rho v = 0) \tag{3}$$

In Equation (3), ρ and v represent the density and velocity vector, respectively.

$$\nabla \cdot \left(\rho \vec{v} \vec{v} \right) = -\nabla p + \nabla \cdot \left(\vec{\tau} \right) + \rho \vec{g} \tag{4}$$

where $\vec{\tau}$ is the stress tensor, p the static pressure, and $\vec{g}$ the direction of the gravitational component. The stress tensor is evaluated as:

$$\vec{\tau} = \mu \left[\left(\nabla \vec{v} + \nabla \vec{v}^{T} \right) - \frac{2}{3} \nabla \cdot \vec{v} I \right] \tag{5}$$

where μ is the molecular viscosity, I is the unit tensor, and the second term on the right-hand side is the effect of volume dilation. The pressure velocity coupling associated with Equations (3) and (4) was handled using the SIMPLE scheme, and the gradients

were evaluated using the Least-Squares Cell-Based option. The various Non-Newtonian viscosity models shown in Table 1 were implemented as user-defined functions in ANSYS FLUENT [18] to compute μ.

The source term for the scalar transport equation for hemolysis prediction in the Eulerian framework listed previously (cf. Equation (2)) was also implemented as a user-defined function. Hemolysis predictions in the Lagrangian framework were made via numerical integration of shear stress and residence time spatial variations under the assumption of fully developed Newtonian fluid flow. Under these conditions, the radial (r) variations in velocity (v) and shear stress (τ) for a circular pipe of radius R are represented as:

$$v(r) = -\frac{1}{4}\frac{\Delta P}{L}(R^2 - r^2) \tag{6}$$

$$\tau(r) = \frac{r}{2}\frac{\Delta P}{L} \tag{7}$$

The pressure gradient ($\Delta P/L$) (where L is the flow length) in Equations (6) and (7) can be expressed as a function of Reynolds number (Re) and average inlet velocity (v_{avg}) as [19]:

$$\frac{\Delta P}{L} = \frac{16}{Re}\rho v_{avg}^2 \tag{8}$$

The stress exposure time t can also be computed based on L and Equation (6) as:

$$t(r) = L/v(r) \tag{9}$$

The radial variations in shear stress and residence time based on Equations (7) and (9) can be employed to compute the radial variations in blood damage D in the power law model as:

$$D(r) = C\tau(r)^b\left[\frac{L}{v(r)}\right]^a \tag{10}$$

Finally, given the assumption of constant density, the blood damage at the outlet in the Lagrangian reference frame can be obtained by integrating across the cross-sectional area A as:

$$D = \frac{\int u(r)D(r)dA}{\int u(r)dA} \tag{11}$$

Table 3 summarizes the cases investigated in this study for the geometries shown in Figure 1.

Table 3. Summary of cases investigated.

Geometry	Viscosity Model	Power Law Constants (Table 2)	Shear Stress Ranges (Pa)	Average Exposure Time (s) Ranges *
Straight capillary tube (hemolysis from inlet to outlet)	Newtonian (0.002 Pa-s, 0.0063 Pa-s), Casson	Blood damage II, III, IV	10–600	5.8×10^{-3}–93×10^{-3}
FDA nozzle forward flow (hemolysis from inlet to outlet across the throat only)	Newtonian (0.0035 Pa-s), 5 Non-Newtonian (Table 1, Figure 3)	Blood damage I	1–20	24×10^{-3}–386×10^{-3}
FDA nozzle reverse flow (hemolysis from inlet to outlet across the throat only)	Newtonian (0.0035 Pa-s), 5 Non-Newtonian (Table 1, Figure 3)	Blood damage I	1–20	24×10^{-3}–386×10^{-3}

* Based on flow path length and inlet velocity.

3. Results and Discussion

3.1. Mesh Convergence and Velocity Profiles

Under fully developed laminar flow conditions for Newtonian fluids, the Darcy friction factor (f_D) has been shown to be equal to 64/Re [19]. Therefore, mesh convergence in the capillary geometry was ensured by predicting the pressure drop and shear stresses at fully developed flow conditions and comparing the predictions against theoretical values [19]. This is shown in Figure 5. It is interesting to see that the results from the Casson model, which show the most deviation from Newtonian behavior at low strain rate conditions (cf. Figure 3), also show similar f_D as Newtonian fluids in this geometry. This is aligned with previous measurements involving Non-Newtonian fluids [20].

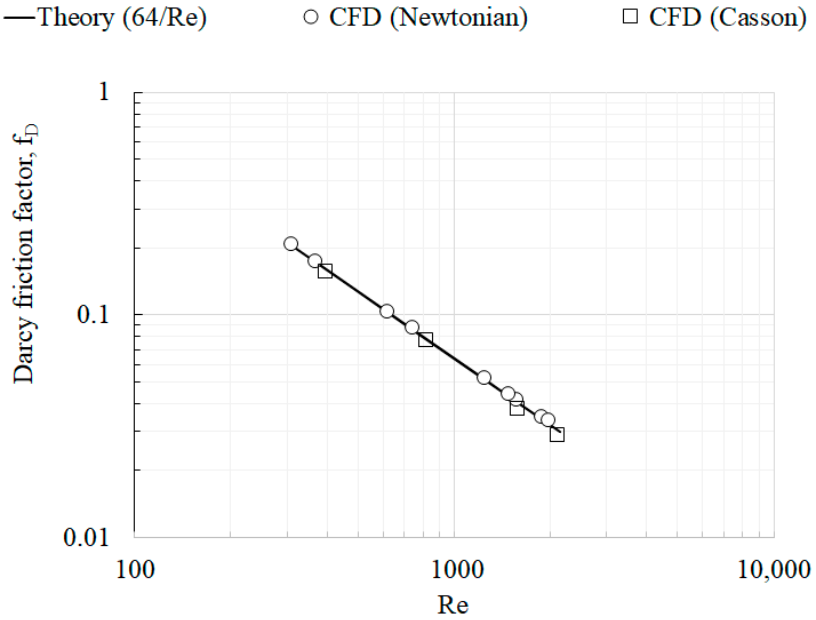


Figure 5. Darcy friction factor (f_D) predictions against theoretical values demonstrating mesh convergence in the capillary tube geometry.

Mesh convergence in the FDA nozzle for the reverse flow direction (Figure 1b) was evaluated for Reynolds numbers 125, 500, and 2000 by modeling blood as a Newtonian fluid and progressively refining the mesh with element counts of 231 K, 439 K, and 966 K. Key solution parameters, including velocity profiles, were monitored to assess sensitivity to mesh density. Refinement was continued until further increases in element count resulted in negligible changes, indicating that the solution reflected the physical behavior rather than mesh-dependent artifacts. As illustrated in Figure 6a–f, the velocity profiles corresponding to different mesh densities overlap almost entirely. This overlap demonstrates that the numerical results remain consistent and are independent of further mesh refinement at the tested Reynolds numbers. The convergence analysis confirms that increasing the mesh density from 231 K to 966 K elements does not significantly alter the velocity profiles, indicating that mesh convergence has been achieved. This ensures the reliability and accuracy of the numerical solution for subsequent analysis, as the results are no longer influenced by discretization errors. Mesh convergence on this identical 966 K mesh, albeit for the forward flow direction (Figure 1c), has been demonstrated in our previous publication [17].

Figure 7 illustrates variations in axial velocity predictions using both Newtonian and Non-Newtonian models under reverse flow conditions along the monitor locations shown in Figure 1b. At low Reynolds numbers, there are distinct differences in the velocity profiles predicted by the different viscosity models. At an axial location of Z = 0.088, the highest peak velocities are predicted by the Newtonian model. This was expected since Newto-

nian fluids do not account for shear-thinning behavior of the fluid, whereas prediction differences from the Non-Newtonian models result from their unique treatment of viscosity dependencies on shear rates (cf. Table 1). The Casson, Cross, and power law models predict the lowest velocities at this axial location at Re 125, resulting from the highest viscosity predicted by these models at low strain rates (cf. Figure 3). However, differences between the models decrease at higher Re when convection starts to dominate momentum diffusion. At an axial location of Z = 0 corresponding to the throat inlet, a nearly uniform velocity profile is obtained across all scenarios (Re, viscosity models). Furthermore, the throat length (0.04 m) is smaller than 0.05 ReD, which is the minimum requirement for achieving fully developed flow at Re 500 and 2000. This will have implications when hemolysis predictions in the Eulerian framework are compared against those in the simplified Lagrangian framework (Equation (11), where a fully developed velocity profile has been assumed.

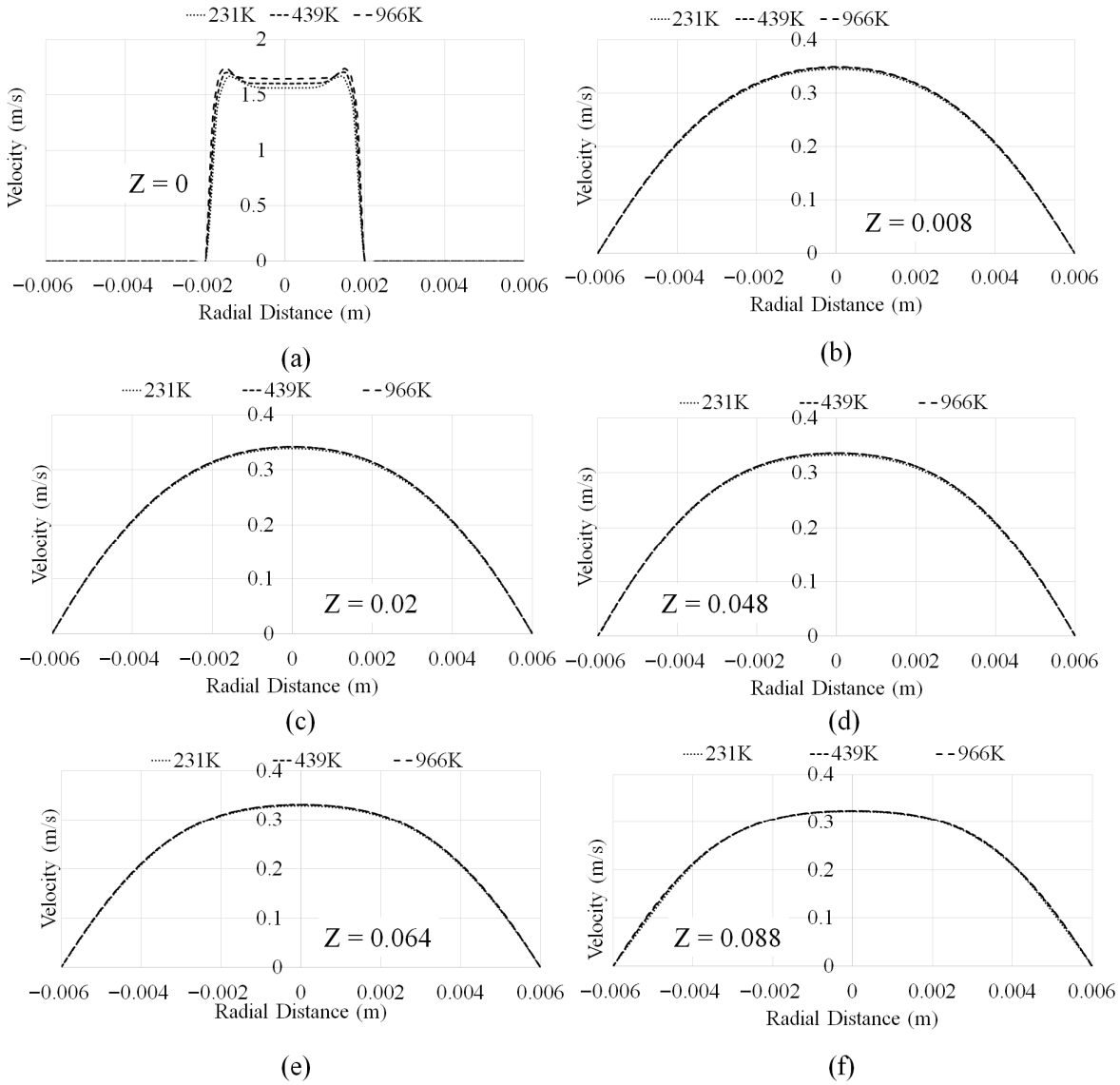


Figure 6. Velocity profiles at different axial locations predicted using different mesh sizes towards demonstrating mesh convergence in the FDA nozzle geometry for reverse flow direction. (**a**) Z = 0; (**b**) Z = 0.008; (**c**) Z = 0.02; (**d**) Z = 0.048; (**e**) Z = 0.064; (**f**) Z = 0.088.

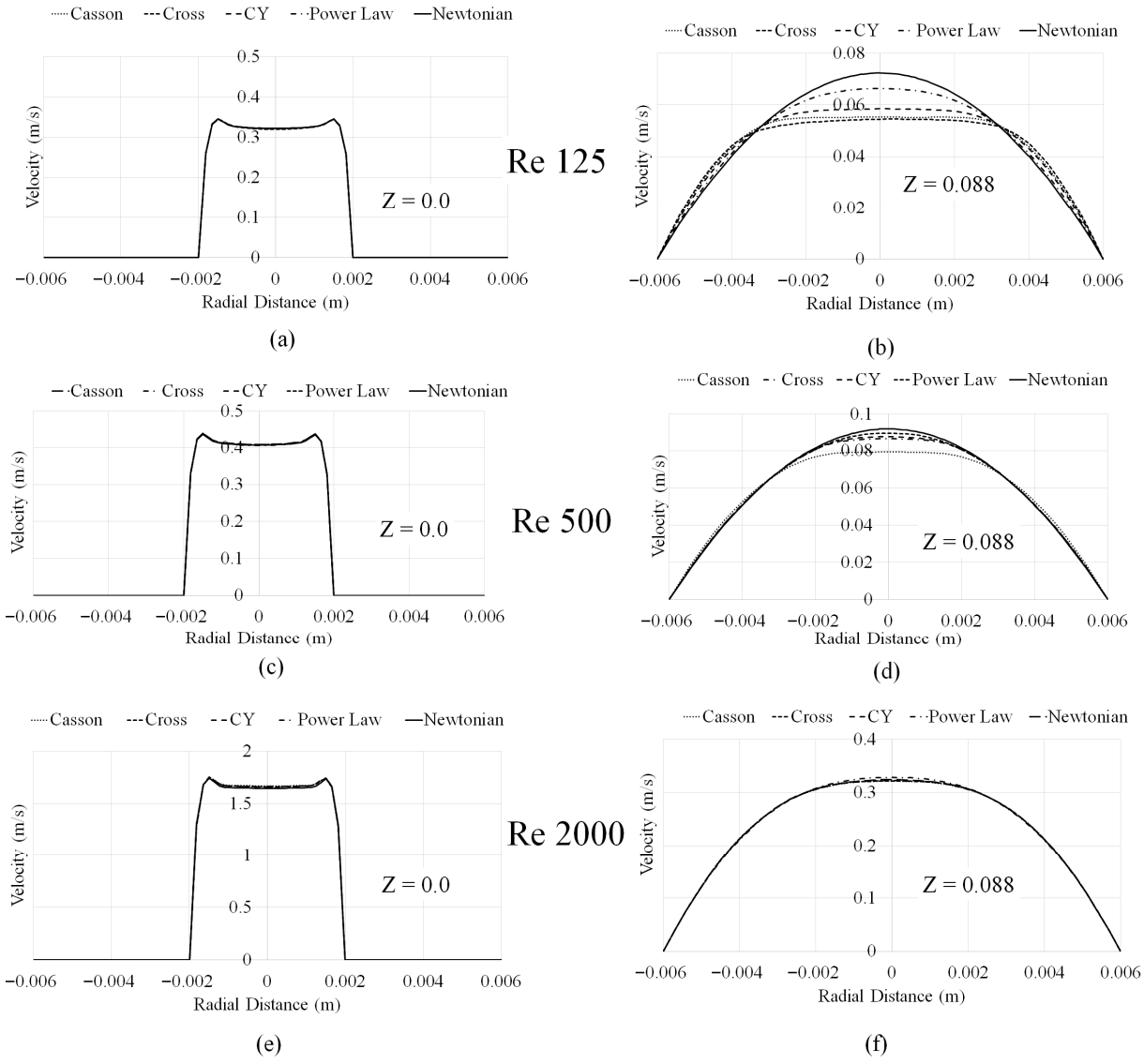


Figure 7. Velocity profiles at different axial locations predicted using different Non-Newtonian models in the FDA nozzle geometry for reverse flow direction. (**a**) Z = 0 (Re 125); (**b**) Z = 0.088 (Re 125); (**c**) Z = 0 (Re 500); (**d**) Z = 0.088 (Re 500); (**e**) Z = 0 (Re 2000); (**f**) Z = 0.088 (Re 2000).

Under laminar flow conditions within the FDA geometry, previous studies have shown that most of the hemolysis occurs due to the high shear stresses at the throat [14,17]. This was confirmed in this study as well, where nearly 80% of the hemolysis was found to occur due to the high shear stresses at the throat wall for both flow directions. Consequently, the average shear stress at the throat wall was employed to compute the Darcy friction factor (f_D) as per Equation (12), and the results are compared against the theoretical value of 64/Re associated with fully developed flow conditions in Figure 8.

$$f_D = \frac{8\tau_{avg}}{\rho v_{avg}^2} \tag{12}$$

Due to steeper velocity gradients at the throat inlet in comparison to the fully developed velocity profile (Figure 7a,c,e), the f_D values for most of the scenarios are a factor of 2–3 higher than the theoretical value.

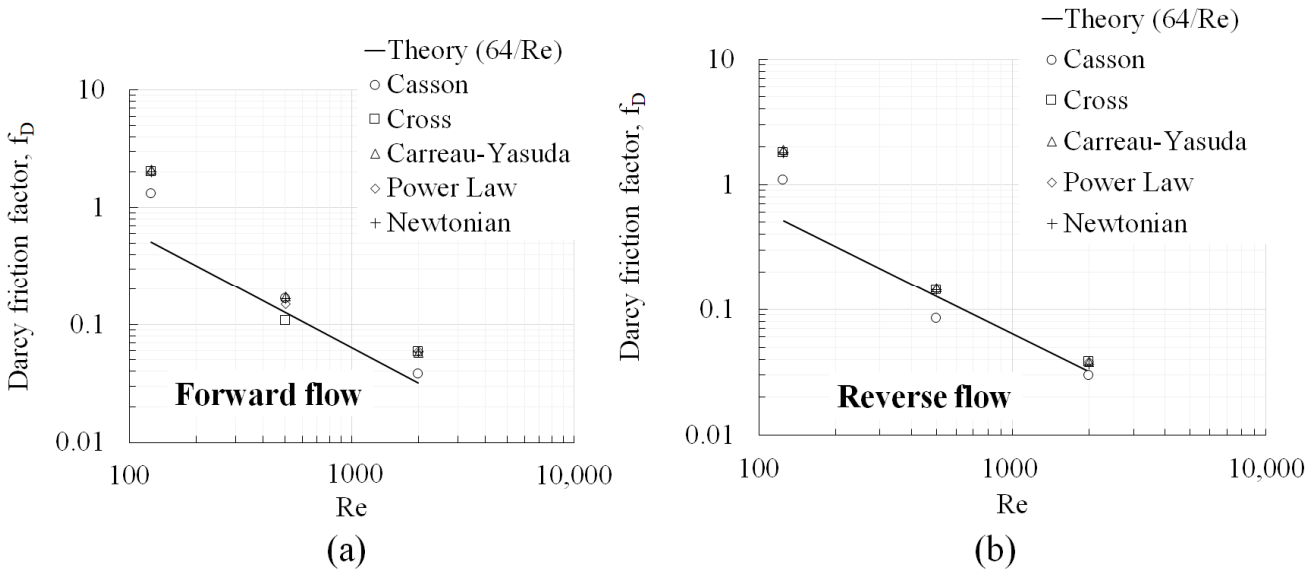


Figure 8. Friction factor in the FDA nozzle: (**a**) Forward flow; (**b**) Reverse flow.

3.2. Hemolysis Assessments

In Figure 9, the absolute values of the blood damage index (D) (cf. Equations (2) and (11)) are shown for the capillary tube geometry. The predictions from the Lagrangian model were scaled (by numbers shown in the legend) to enable representation on the same graph for relative hemolysis predictions. While the absolute values of D are sensitive to the hemolysis coefficients (cf. Table 3) employed in the simulations, the relative hemolysis variations show the same trends. Further, when fully developed flow conditions persist throughout the capillary tube geometry, *absolute* hemolysis predictions in both Eulerian and Lagrangian formulations remain proportional to each other and are independent of the blood viscosity model or the hemolysis power law coefficients. However, the value of the proportionality constant (the number to which the Lagrangian values are scaled, as indicated in the legends) is specific to the power law coefficients employed in the analysis. The value of the proportionality constant is also different for the Newtonian (Figure 9a) and Casson viscosity models (Figure 9b). However, the relative variations are independent of the viscosity model as shown in Figure 9c. Recent studies [7] have suggested that the erroneous treatment of residence time in the Eulerian formulation resulting from flow acceleration and recirculation may necessitate the formulation/deduction of separate sets of coefficients for each of the Eulerian and Lagrangian formulations. However, the results from this study suggest that this requirement may be alleviated for relative hemolysis assessments in simple geometries when the conditions of fully developed flow are present, since Eulerian and Lagrangian absolute hemolysis predictions are simply proportional to each other. Also, considering the challenges with obtaining a converged solution to relative hemolysis in the Lagrangian framework as mentioned previously (i.e., generating an adequate number of flow pathlines), these results suggest that under conditions of fully developed flow, the Eulerian framework may still be employed for relative hemolysis assessments irrespective of the hemolysis power law or viscosity model employed.

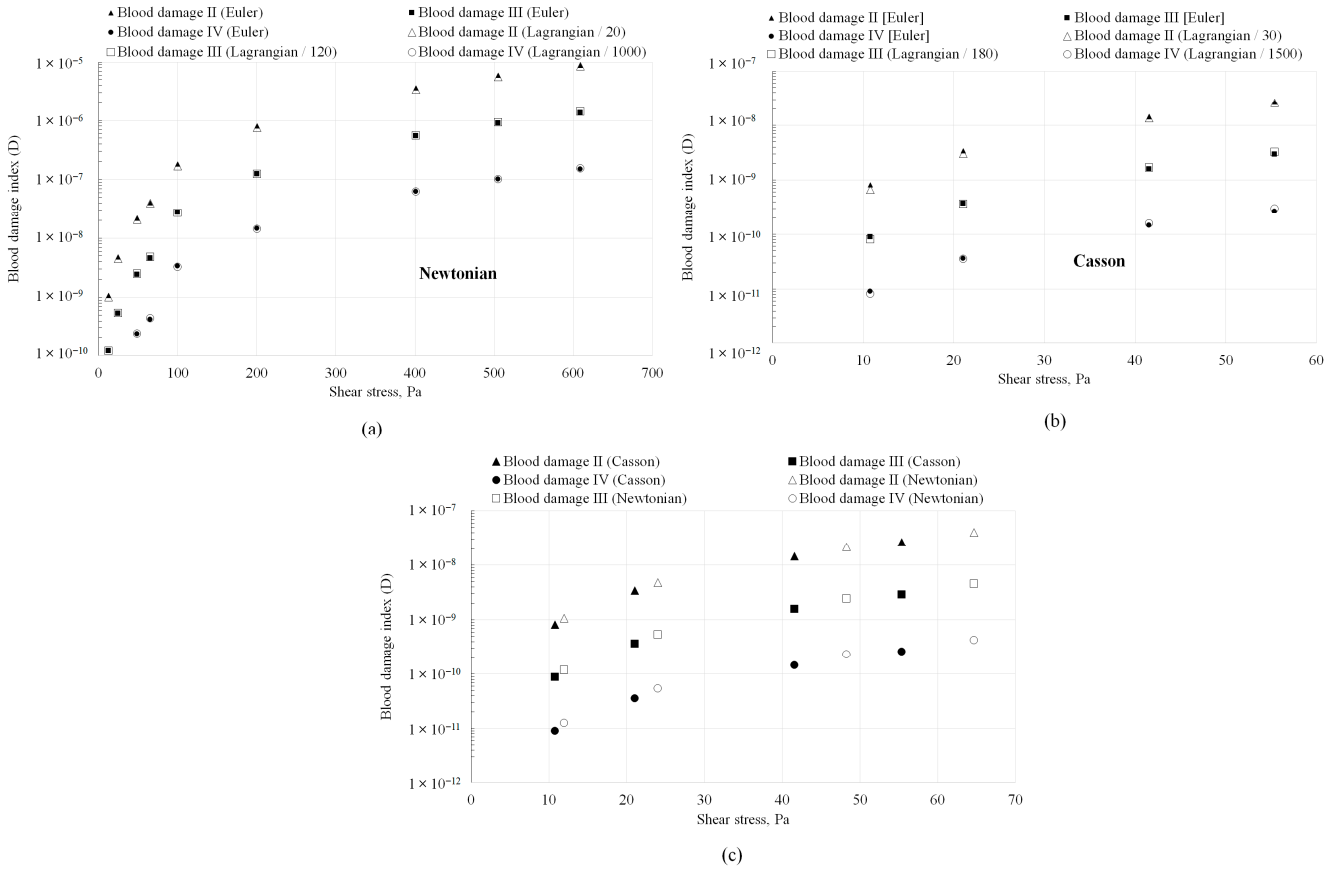


Figure 9. Eulerian and Lagrangian blood damage index predictions in the capillary tube. The hemolysis constants corresponding to different blood damage models are listed in Table 2. (**a**) Newtonian viscosity model; (**b**) Casson viscosity model; (**c**) Newtonian and Casson models.

The absolute values of the blood damage index predicted by the Eulerian framework (cf. Equation (2)) across the throat of the FDA nozzle geometry are shown in Figure 10. First, except for the Casson model, the absolute hemolysis predictions are relatively insensitive to the viscosity model employed. Second, in contrast to previous studies [5], the forward flow direction (cf. Figure 1c) results in higher blood damage than reverse flow, with the impact of flow direction becoming more significant at higher Reynolds numbers. This may be attributed to the differences in velocity profiles across the throat section for the two scenarios. Although the incoming throat velocity is nearly uniform across all Re (cf. Figure 7a,c,e), the flow becomes fully developed after a throat length of 0.025 m (0.05 ReD) at Re 125. Consequently, the blood damage index results are relatively insensitive (less than 1% variation) to the flow direction at Re 125. However, as Re increases, the entrance length for fully developed flow increases and the differences in the velocity profiles resulting from the flow direction contribute to increasing the difference in the blood damage index. This is confirmed in Figure 11, where the average wall shear stresses at the throat wall are shown. Again, except for the Casson model, the results are insensitive to the viscosity model employed. The fact that the prediction differences resulting from flow direction increase with Re indicates that this is due to velocity profile differences between the two scenarios.

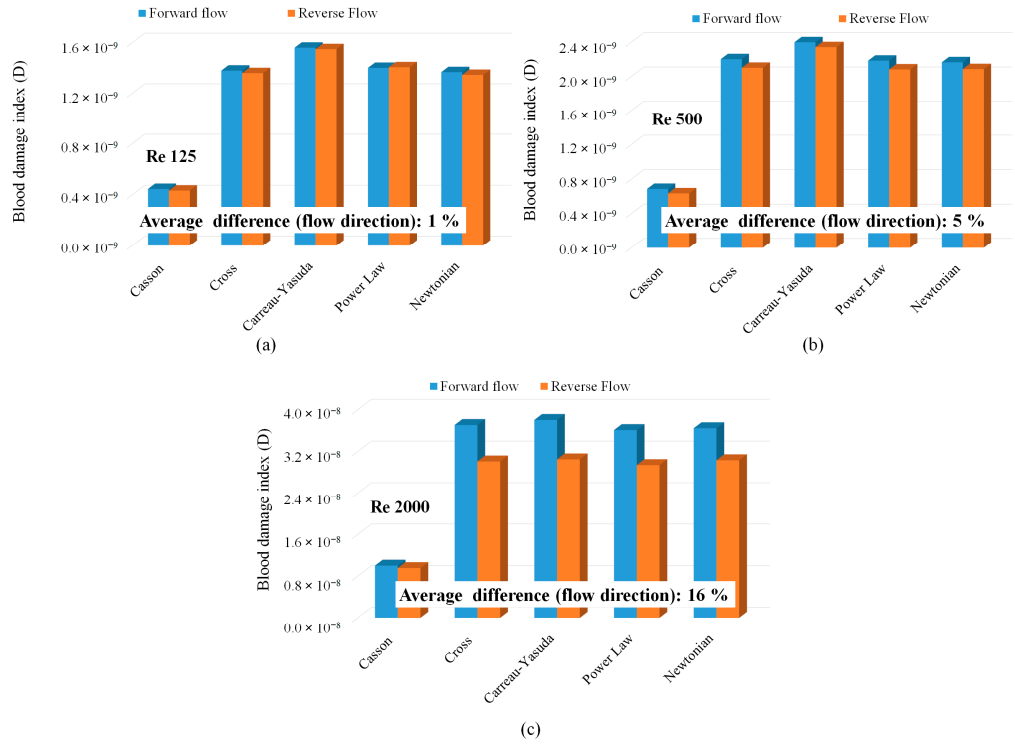


Figure 10. Absolute values of the blood damage index predicted by the Eulerian framework across the throat of the FDA nozzle geometry. (**a**) Re 125; (**b**) Re 500; (**c**) Re 2000. Prediction differences resulting from the flow direction are also shown.

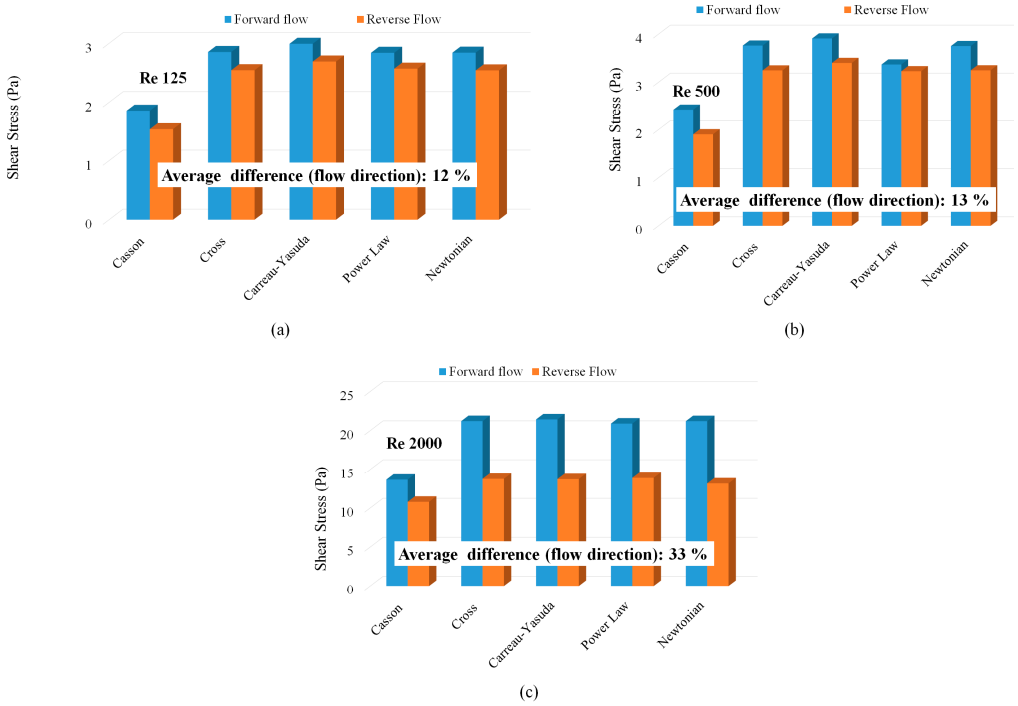


Figure 11. Average shear stresses at the throat of the FDA nozzle geometry. (**a**) Re 125; (**b**) Re 500; (**c**) Re 2000. Prediction differences resulting from the flow direction are also shown.

To assess how these deviations from fully developed flow velocity profiles impact relative hemolysis predictions, all of the blood damage index predictions (for both flow directions) obtained from the Eulerian framework (cf. Figure 10) are shown in Figure 12a, along with scaled values obtained from the simplified Lagrangian framework (Equation (11))

where a fully developed velocity profile and Newtonian viscosity has been assumed. Since only three values of Re (125, 500, and 2000) were considered in this geometry, blood damage predictions at other intermediate Re were also made using the simplified Lagrangian framework. It is interesting to note that even when developing flow conditions do not persist throughout the geometry, identical variations in relative hemolysis are observed in both the Eulerian and Lagrangian frameworks. In addition, this variation is independent of the viscosity model employed.

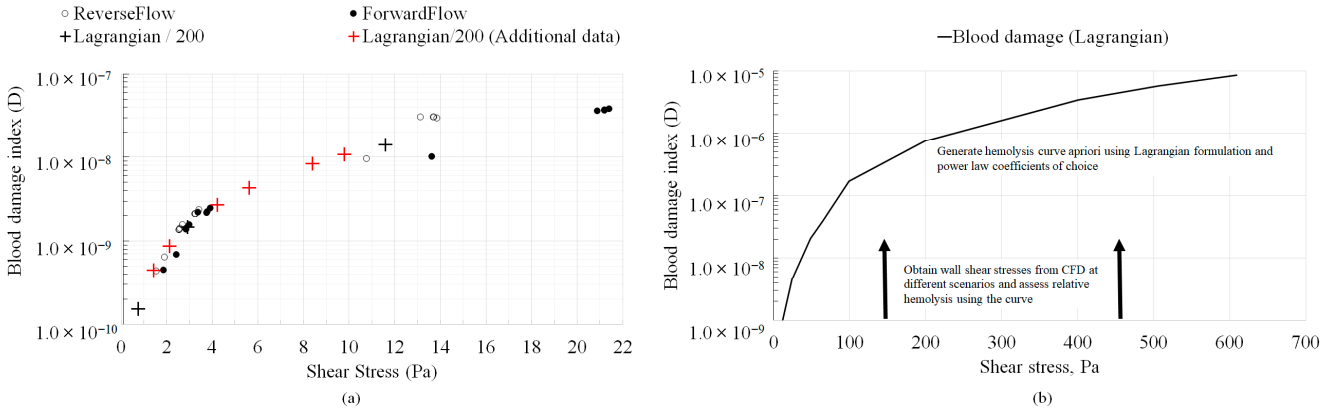


Figure 12. (**a**) Eulerian and Lagrangian blood damage index predictions in the FDA nozzle; (**b**) strategy for relative hemolysis assessment using the simplified Lagrangian model (Equation (11)).

Therefore, in simple geometries similar to the ones investigated in this study (capillary tubes, FDA benchmark nozzle), where hemolysis is dominated by wall shear, the aforementioned Lagrangian hemolysis modeling methodology that is formulated based on fully developed Newtonian fluid flow could be employed as a surrogate for quick relative hemolysis assessments. This could be done by generating an absolute hemolysis versus shear stress curve a priori (based on Equations (6)–(11)) using any set of power law coefficients of choice, as shown in Figure 12b. Next, if fully developed flow conditions are thought to persist throughout the geometry, then wall shear stress values could be estimated based on average inlet velocity and Re from Equation (7). If not, wall-averaged shear stress can be obtained from CFD simulations for different design prototypes or flow situations and relative hemolysis assessments made based on this curve (cf. Figure 12b).

Although only laminar flow conditions were explored in this study, the range of wall shear stresses investigated in this study (1–600 Pa, cf. Table 3) is within the ranges found in many anatomical regions and device geometries, including pumps, heart valves, and coronary arteries and stents [21]. Furthermore, the study indicated that a significant amount of the blood volume within these devices does not experience shear stress greater than 50 Pa [21].

While two geometries with fully developed flow and developing flow conditions were assessed in this study, the extension of the proposed methodology for relative hemolysis assessments in more complicated and clinically relevant device geometries, such as blood pumps and heart valves, needs to be undertaken. Such geometries may have localized fluid recirculation zones where cell shear stress exposure times may not be accurately represented by the steady-state, fully developed Lagrangian flow framework proposed in this study [22]. Second, the assumption of a fully developed flow in the Lagrangian framework inherently assumes that the shear stress is maximum at the wall. However, there may be scenarios where hemolysis may be induced by flow or small-scale eddies. In such turbulent scenarios, the modeling of the effective shear stresses experienced by the RBCs is critical and could be undertaken by using the computed energy dissipation terms, for instance [23]. Hemolysis occurs as a result of a cascade of processes involving

platelet margination, adhesion, aggregation, and cohesion that may not be adequately represented by simplistic power law models/coefficients that were generated using shear devices. Therefore, more mechanistic models of hemolysis where cell deformation occurs also need to be considered, where the power law model may not be applicable [24]. A direct extension of the results of this study to thrombus prediction in vivo scenarios is challenging. While the complex hydrodynamic interactions between deformable RBCs, ellipsoid platelets, and a model thrombus have been simulated and compared against in vivo data from mouse models [25] and significant advances have been made in the modeling of coagulation, platelet deposition, aggregation, and embolization, developing patient-specific models capable of predicting the transient process of thrombus formation and embolism under in vivo conditions remains a challenge [26].

4. Conclusions

The goal of this paper is to enable rapid assessments and predictions of *relative* hemolysis for quickly evaluating device design prototypes. Towards achieving this objective, absolute hemolysis predictions in an Eulerian framework were first generated from computational fluid dynamic (CFD) simulations under laminar flow conditions encompassing five blood viscosity models, four sets of hemolysis power law coefficients, fully developed as well as developing velocity flow conditions, and a wide range of shear stresses (1–600 Pa), strain rates (1–10,000 s^{-1}), and stress exposure times (5–400 milliseconds). Corresponding absolute hemolysis predictions were also obtained in an expedient manner in a Lagrangian framework via numerical integration of shear stress and residence time spatial variations under the assumption of fully developed Newtonian fluid flow. Based on the results of this study, the following conclusions may be drawn:

1. At laminar, fully developed flow conditions, both Newtonian and Non-Newtonian models showed identical shear stress variations with Reynolds number.
2. When fully developed flow conditions persist throughout the geometry, *absolute* hemolysis predictions (in both Eulerian and Lagrangian formulations) were proportional to each other and independent of the blood viscosity model or the hemolysis power law coefficients. However, the value of the proportionality constant was specific to the power law coefficients employed in the analysis. The value of the proportionality constant was also different for the Casson non-viscosity model.
3. While recent studies [7] have suggested that the erroneous treatment of residence time in the Eulerian formulation (resulting from flow acceleration) may necessitate the formulation/deduction of separate sets of coefficients for each (Eulerian/Lagrangian) formulation, the results from this study suggest that this requirement may be alleviated for relative hemolysis assessments when the conditions of fully developed flow are present, since Eulerian and Lagrangian absolute hemolysis predictions are simply proportional to each other.
4. Even when developing flow conditions persist throughout the geometry, identical variations in absolute hemolysis as a function of wall shear stresses were observed between the Eulerian and Lagrangian frameworks that were generally independent of the viscosity model. Therefore, in simple geometries similar to the ones investigated in this study (capillary tubes, FDA benchmark nozzle), where hemolysis is dominated by wall shear and hemolysis in recirculation regions is absent, the simplified Lagrangian hemolysis modeling methodology formulated based on fully developed Newtonian fluid flow could be employed as a surrogate for quick relative hemolysis assessments. This could be done by generating an absolute hemolysis versus shear stress curve a priori using any set of power law coefficients of choice. Next, wall shear stress

values could be obtained from CFD simulations for different design prototypes or flow situations and relative hemolysis assessments made based on the curve.

Author Contributions: This article was published with contributions from the following individuals: conceptualization, N.G. and G.K.; methodology, N.G. and G.K.; formal analysis.; N.G., R.W., G.G.; investigation: N.G., R.W., G.G.; writing—original draft preparation, N.G.; writing—review and editing, G.K.; visualization, N.G., R.W., G.G.; supervision, G.K. All authors have read and agreed to the published version of the manuscript.

Funding: This research received no external funding.

Data Availability Statement: All data that is relevant to this study is contained within the article. Any additional supplemental information that is needed is available upon request from the corresponding author.

Conflicts of Interest: The authors declare no conflicts of interest.

References

1. Kameneva, M.V.; Burgreen, G.W.; Kono, K.; Repko, B.; Antaki, J.F.; Umezu, M. Effects of turbulent stresses upon mechanical hemolysis: Experimental and computational analysis. *ASAIO J.* **2004**, *50*, 418–423. [CrossRef]
2. Hariharan, P.; Giarra, M.; Reddy, V.; Day, S.; Manning, K.B.; Deutsch, S.; Stewart, S.F.C.; Myers, M.R.; Berman, M.R.; Burgreen, G.W.; et al. Experimental particle image velocimetry protocol and results database for validating computational fluid dynamic simulations of the FDA benchmark nozzle model. *J. Biomech. Eng.* **2011**, *133*, 041002. [CrossRef]
3. Stewart, S.F.C.; Hariharan, P.; Paterson, E.G.; Burgreen, G.W.; Reddy, V.; Day, S.W.; Giarra, M.; Manning, K.B.; Deutsch, S.; Berman, M.R.; et al. Results of FDA's First Interlaboratory Computational Study of a Nozzle with a Sudden Contraction and Conical Diffuser. *Cardiovasc. Eng. Technol.* **2013**, *4*, 374–391. [CrossRef]
4. Stewart, S.F.C.; Paterson, E.G.; Burgreen, G.W.; Hariharan, P.; Giarra, M.; Reddy, V.; Day, S.W.; Manning, K.B.; Deutsch, S.; Berman, M.R.; et al. Assessment of CFD performance in simulations of an idealized medical device: Results of FDA's first computational Interlaboratory study. *Cardiovasc. Eng. Technol.* **2012**, *3*, 139–160. [CrossRef]
5. Herbertson, L.H.; Olia, S.E.; Daly, A.; Noatch, C.P.; Smith, W.A.; Kameneva, M.V.; Malinauskas, R.A. Multilaboratory study of flow-induced Hemolysis using the FDA benchmark nozzle model. *Artif. Organs* **2014**, *39*, 237–248. [CrossRef]
6. Mantegazza, A.; Tobin, N.; Manning, K.B.; Craven, B.A. Examining the universality of the hemolysis power law model from simulations of the FDA nozzle using calibrated model coefficients. *Biomech. Model. Mechanobiol.* **2023**, *22*, 433–451. [CrossRef]
7. Faghih, M.M.; Craven, B.A.; Sharp, M.K. Practical implications of the erroneous treatment of exposure time in the Eulerian hemolysis power law model. *Artif. Organs* **2023**, *47*, 1531–1538. [CrossRef]
8. Menon, K.; Hu, Z.; Marsden, A.L. Cardiovascular fluid dynamics: A journey through our circulation. *Flow* **2024**, *4*, E7. [CrossRef]
9. Kopernik, M. Modelling of blood thrombosis at microscopic and mesoscopic scales. *Comput. Assist. Methods Eng. Sci.* **2019**, *25*, 21–45.
10. Giersiepen, M.; Wurzinger, L.J.; Opitz, R.; Reul, H. Estimation of shear stress-related blood damage in heart valve prostheses-in vitro comparison of 25 aortic valves. *Int. J. Artif. Organs* **1990**, *13*, 300–306. [CrossRef]
11. Craven, B.A.; Aycock, K.I.; Herbertson, L.H.; Malinauskas, R.A. A CFD-based Kriging surrogate modeling approach for predicting device-specific hemolysis power law coefficients in blood-contacting medical devices. *Biomech. Model. Mechanobiol.* **2019**, *18*, 1005–1030. [CrossRef] [PubMed]
12. Stiehm, M.; Wüstenhagen, C.; Siewert, S.; Grabow, N.; Schmitz, K.P. Numerical simulation of pulsatile flow through a coronary nozzle model based on FDA's benchmark geometry. *Curr. Dir. Biomed. Eng.* **2017**, *3*, 775–778. [CrossRef]
13. Good Bryan, C. The Effects of non-Newtonian Blood Modeling and Pulsatility on Hemodynamics in the Food and Drug Administration's Benchmark Nozzle Model. *Biorheology* **2023**, *59*, 1–18. [CrossRef]
14. Trias, M.; Arbona, A.; Massó, J.; Miñano, B.; Bona, C. FDA's nozzle numerical simulation challenge: Non-Newtonian fluid effects and blood damage. *PLoS ONE* **2014**, *9*, e92638. [CrossRef]
15. Hussein, B.K.; Al-Azawy, M.G.; Al-Waaly, A.A.; Hamza, Z.A. Evaluation of Turbulence and Non-Newtonian Blood Rheology Models Through FDA Nozzle. In Proceedings of the 2021 International Conference on Advance of Sustainable Engineering and its Application (ICASEA), Wasit, Iraq, 27–28 October 2021; IEEE: New York, NY, USA, 2021; pp. 1–5.
16. Zakaria, M.S.; Zainudin, S.H.; Abdullah, H.; Yuan, C.S.; Abd Latif, M.J.; Osman, K. CFD Simulation of Non-Newtonian Effect on Hemodynamics Characteristics of Blood Flow through Benchmark Nozzle. *J. Adv. Res. Fluid Mech. Therm. Sci.* **2019**, *64*, 117–125.
17. Krishnamoorthy, G.; Gholizadeh, N. Blood Damage Analysis within the FDA Benchmark Nozzle Geometry at Laminar Conditions: Prediction Sensitivities to Software and Non-Newtonian Viscosity Models. *Symmetry* **2024**, *16*, 1165. [CrossRef]
18. ANSYS Inc. ANSYS Fluent. *Version 2023 R2.* 2023. Available online: https://www.ansys.com/products/fluids/ansys-fluent (accessed on 1 January 2024).

19. McCabe, W.L.; Smith, J.C.; Harriott, P. *Unit Operations of Chemical Engineering*; McGraw-Hill: New York, NY, USA, 1967; Volume 5.
20. Metzner, A.B.; Reed, J.C. Flow of non-newtonian fluids—Correlation of the laminar, transition, and turbulent-flow regions. *Aiche J.* **1955**, *1*, 434–440. [CrossRef]
21. Hong, J.K.; Gao, L.; Singh, J.; Goh, T.; Ruhoff, A.M.; Neto, C.; Waterhouse, A. Evaluating medical device and material thrombosis under flow: Current and emerging technologies. *Biomater. Sci.* **2020**, *8*, 5824–5845. [CrossRef]
22. Taskin, M.E.; Fraser, K.H.; Zhang, T.; Wu, C.; Griffith, B.P.; Wu, Z.J. Evaluation of Eulerian and Lagrangian models for hemolysis estimation. *ASAIO J.* **2012**, *58*, 363–372. [CrossRef]
23. Wu, P.; Gao, Q.; Hsu, P.L. On the representation of effective stress for computing hemolysis. *Biomech. Model. Mechanobiol.* **2019**, *18*, 665–679. [CrossRef]
24. Fogelson, A.L.; Neeves, K.B. Fluid mechanics of blood clot formation. *Annu. Rev. Fluid Mech.* **2015**, *47*, 377–403. [CrossRef] [PubMed]
25. Wang, W.; Diacovo, T.G.; Chen, J.; Freund, J.B.; King, M.R. Simulation of platelet, thrombus and erythrocyte hydrodynamic interactions in a 3D arteriole with in vivo comparison. *PLoS ONE* **2013**, *8*, e76949. [CrossRef] [PubMed]
26. Hosseinzadegan, H.; Tafti, D.K. Modeling thrombus formation and growth. *Biotechnol. Bioeng.* **2017**, *114*, 2154–2172. [CrossRef] [PubMed]

Disclaimer/Publisher's Note: The statements, opinions and data contained in all publications are solely those of the individual author(s) and contributor(s) and not of MDPI and/or the editor(s). MDPI and/or the editor(s) disclaim responsibility for any injury to people or property resulting from any ideas, methods, instructions or products referred to in the content.